



UvA-DARE (Digital Academic Repository)

Search for the neutral Higgs boson at LEP

Adeva, B.; Adriani, O.; Aguilar-Benitez, M.; Ahlen, S.P.; Akbari, H.; Alcaraz, J.; Aloisio, A.; Alverson, G.; Linde, F.L.

Published in:
Physics Letters B

DOI:
[10.1016/0370-2693\(92\)90047-8](https://doi.org/10.1016/0370-2693(92)90047-8)

[Link to publication](#)

Citation for published version (APA):

Adeva, B., Adriani, O., Aguilar-Benitez, M., Ahlen, S. P., Akbari, H., Alcaraz, J., ... Linde, F. L. (1992). Search for the neutral Higgs boson at LEP. *Physics Letters B*, 283, 454-464. DOI: 10.1016/0370-2693(92)90047-8

General rights

It is not permitted to download or to forward/distribute the text or part of it without the consent of the author(s) and/or copyright holder(s), other than for strictly personal, individual use, unless the work is under an open content license (like Creative Commons).

Disclaimer/Complaints regulations

If you believe that digital publication of certain material infringes any of your rights or (privacy) interests, please let the Library know, stating your reasons. In case of a legitimate complaint, the Library will make the material inaccessible and/or remove it from the website. Please Ask the Library: <http://uba.uva.nl/en/contact>, or a letter to: Library of the University of Amsterdam, Secretariat, Singel 425, 1012 WP Amsterdam, The Netherlands. You will be contacted as soon as possible.

Search for the neutral Higgs boson at LEP

L3 Collaboration

B. Adeva^a, O. Adriani^b, M. Aguilar-Benitez^c, S. Ahlen^d, H. Akbari^e, J. Alcaraz^c, A. Aloisio^f, G. Alverson^g, M.G. Alviggi^h, G. Ambrosi^h, Q. Anⁱ, H. Anderhub^j, A.L. Anderson^k, E.W. Anderson^l, V.P. Andreev^m, T. Angelov^k, L. Antonovⁿ, D. Antreasyan^o, P. Arce^c, A. Arefiev^p, A. Atamanchuk^m, T. Azemoon^q, T. Aziz^{r,s}, P.V.K.S. Baba^l, P. Bagnaia^l, J.A. Bakken^u, L. Baksay^v, R.C. Ball^q, S. Banerjee^r, J. Bao^c, R. Barillère^a, L. Barone^l, R. Battiston^h, A. Bay^w, F. Becattini^b, U. Becker^{k,j}, F. Behner^j, J. Behrens^j, S. Beingssner^x, Gy.L. Bencze^y, J. Berdugo^c, P. Berges^k, B. Bertucci^h, B.L. Betev^{n,j}, M. Biasini^h, A. Biland^j, G.M. Bilei^h, R. Bizzarri^l, J.J. Blaising^x, P. Blömeke^s, B. Blumenfeld^c, G.J. Bobbink^z, M. Bocciolini^b, R. Bock^s, A. Böhm^s, B. Borgia^l, D. Bourilkovⁿ, M. Bourquin^w, D. Boutigny^x, B. Bouwens^z, E. Brambilla^f, J.G. Branson^{aa}, I.C. Brock^{ab}, M. Brooks^{ac}, F. Bruyart^a, C. Buisson^{ad}, A. Bujak^{ac}, J.D. Burger^k, W.J. Burger^w, J.P. Burq^{ad}, J. Busenitz^v, X.D. Cai^l, M. Capell^{af}, M. Caria^h, F. Carminati^b, A.M. Cartacci^b, M. Cerrada^c, F. Cesaroni^l, Y.H. Chang^k, U.K. Chaturvedi^l, M. Chemarin^{ad}, A. Chen^{ag}, C. Chen^{ah}, G.M. Chen^{ah}, H.F. Chen^{ai}, H.S. Chen^{ah}, J. Chen^k, M. Chen^k, M.L. Chen^q, W.Y. Chen^l, G. Chiefari^f, C.Y. Chien^c, M. Chmeissani^q, S. Chung^k, C. Civinini^b, I. Clare^k, R. Clare^k, T.E. Coan^{ac}, H.O. Cohn^{ai}, G. Coignet^s, N. Colino^a, A. Contin^{o,a}, F. Crijns^{ak}, X.T. Cui^l, X.Y. Cui^l, T.S. Dai^k, R. D'Alessandro^b, R. de Asmundis^l, A. Degré^s, K. Deiters^k, E. Dénes^y, P. Denes^u, F. DeNotaristefani^l, M. Dhina^j, D. DiBitonto^v, M. Diemoz^l, H.R. Dimitrovⁿ, C. Dionisi^{l,a}, M.T. Dova^l, E. Drago^f, T. Driever^{ak}, D. Duchesneau^w, P. Duinker^z, I. Duran^c, H. El Mamouni^{ad}, A. Engler^{ab}, F.J. Eppling^k, F.C. Erné^z, P. Extermann^w, R. Fabbretti^{ak}, M. Fabre^j, S. Falciano^l, S.J. Fan^{am}, O. Fackler^{af}, J. Fay^{ad}, M. Felcini^a, T. Ferguson^{ab}, D. Fernandez^c, G. Fernandez^c, F. Ferroni^l, H. Fesefeldt^s, E. Fiandrini^h, J. Field^w, F. Filthaut^{ak}, G. Finocchiaro^l, P.H. Fisher^c, G. Forconi^w, T. Foreman^z, K. Freudenreich^j, W. Friebel^{an}, M. Fukushima^k, M. Gaillard^{ao}, Yu. Galaktionov^{p,k}, E. Gallo^b, S.N. Ganguli^r, P. Garcia-Abia^c, S.S. Gau^{ag}, D. Gele^{ad}, S. Gentile^{l,a}, S. Goldfarb^q, Z.F. Gong^{ai}, E. Gonzalez^c, P. Göttlicher^s, D. Goujon^w, G. Gratta^{ap}, C. Grinnell^k, M. Gruenewald^{ap}, C. Gu^l, M. Guanziroli^l, J.K. Guo^{am}, A. Gurtu^{ra}, H.R. Gustafson^q, L.J. Gutay^{ac}, K. Hangarter^s, A. Hasan^l, D. Hauschildt^z, C.F. He^{am}, T. Hebbeker^s, M. Hebert^{aa}, G. Herten^k, U. Herten^s, A. Hervé^a, K. Hilgers^s, H. Hofer^j, H. Hoorani^l, G. Hu^l, G.Q. Hu^{am}, B. Ille^{ad}, M.M. Ilyas^l, V. Innocente^{fa}, H. Janssen^a, S. Jezequel^s, B.N. Jin^{ah}, L.W. Jones^q, A. Kasser^{ao}, R.A. Khan^l, Yu. Kamyshev^{aj}, P. Kapinos^m, J.S. Kapustinsky^{ac}, Y. Karyotakis^{a,s}, M. Kaur^l, S. Khokhar^l, M.N. Kienzle-Focacci^w, W.W. Kinnison^{ac}, D. Kirkby^{ap}, S. Kirsch^{an}, W. Kittel^{ak}, A. Klimentov^{k,p}, A.C. König^{ak}, O. Kornadt^s, V. Koutsenko^{k,p}, A. Koulbardi^m, R.W. Kraemer^{ab}, T. Kramer^k, V.R. Krastevⁿ, W. Krenz^s, A. Krivshich^m, J. Krizmanic^c, K.S. Kumar^{aq}, V. Kumar^l, A. Kunin^{aq,p}, G. Landi^b, K. Lanius^a, D. Lanske^s, S. Lanzano^f, P. Lebrun^{ad}, P. Lecomte^j, P. Lecoq^a, P. Le Coultre^j, D.M. Lee^{ac}, I. Leedom^g, J.M. Le Goff^a, L. Leistam^a, R. Leiste^{an}, M. Lenti^b, E. Leonardi^l, J. Lettry^j, X. Leytens^z, C. Li^{ai,j}, H.T. Li^{ah}, P.J. Li^{am}, X.G. Li^{ah}, J.Y. Liao^{am}, W.T. Lin^{ag}, Z.Y. Lin^{ai}, F.L. Linde^{az}, B. Lindemann^s, D. Linnhofer^j, L. Lista^f, Y. Liu^l, W. Lohmann^{an,am}, E. Longo^l, Y.S. Lu^{ah}, J.M. Lubbers^a, K. Lübelmeyer^s, C. Luci^a, D. Luckey^{o,k}, L. Ludovici^l

L. Luminari ^l, W.G. Ma ^{ai}, M. MacDermott ^j, P.K. Malhotra ^{r,l}, R. Malik ^l, A. Malinin ^{x,p},
 C. Mañá ^c, D.N. Mao ^q, Y.F. Mao ^{ah}, M. Maolinbay ^j, P. Marchesini ^j, F. Marion ^x, A. Marin ^r,
 J.P. Martin ^{ad}, L. Martinez-Laso ^a, F. Marzano ^l, G.G.G. Massaro ^z, T. Matsuda ^k,
 K. Mazumdar ^r, P. McBride ^{aq}, T. McMahon ^{ac}, D. McNally ^j, Th. Meinholz ^s, M. Merk ^{ak},
 L. Merola ^f, M. Meschini ^b, W.J. Metzger ^{ak}, Y. Mi ^l, G.B. Mills ^{ac}, Y. Mir ^l, G. Mirabelli ^l,
 J. Mnich ^s, M. Möller ^s, B. Monteleoni ^b, R. Morand ^s, S. Morganti ^l, N.E. Moulai ^l,
 R. Mount ^{ap}, S. Müller ^s, A. Nadtochy ^m, E. Nagy ^s, M. Napolitano ^f, H. Newman ^{ap}, C. Neyer ^j,
 M.A. Niaz ^l, L. Niessen ^s, H. Nowak ^{an}, G. Organtini ^l, D. Pandoulas ^s, S. Paoletti ^b,
 G. Passaleva ^b, S. Patricelli ^f, M. Pauluzzi ^h, F. Pauss ^l, Y.J. Pei ^s, D. Perret-Gallix ^x, J. Perrier ^w,
 A. Pevsner ^c, M. Pieri ^{a,b}, P.A. Piroué ^u, E. Plasil ^{aj}, V. Plyaskin ^p, M. Pohl ^j, V. Pojidaev ^{p,b},
 N. Produit ^w, J.M. Qian ^q, K.N. Qureshi ⁱ, R. Raghavan ^r, G. Rahal-Callot ^j, G. Raven ^z,
 P. Razis ^{ar}, K. Read ^{aj}, D. Ren ^j, Z. Ren ^l, M. Rescigno ^l, S. Reucroft ^g, A. Ricker ^s,
 S. Riemann ^{an}, O. Rind ^q, H.A. Rizvi ^l, B.P. Roe ^q, M. Röhner ^s, S. Röhner ^s, L. Romero ^c,
 J. Rose ^s, S. Rosier-Lees ^x, R. Rosmalen ^{ak}, Ph. Rosselet ^{ao}, A. Rubbia ^k, J.A. Rubio ^{a,c},
 H. Rykaczewski ^j, M. Sachwitz ^{an,a}, J. Salicio ^{a,c}, J.M. Salicio ^c, G.S. Sanders ^{ac}, A. Santocchia ^h,
 M.S. Sarakinos ^k, G. Sartorelli ^{o,i}, G. Sauvage ^x, V. Schegelsky ^m, K. Schmiemann ^s,
 D. Schmitz ^s, P. Schmitz ^s, M. Schneegans ^x, H. Schopper ^{as}, D.J. Schotanus ^{ak}, S. Shotkin ^k,
 H.J. Schreiber ^{an}, J. Shukla ^{ab}, R. Schulte ^s, S. Schulte ^s, K. Schultze ^s, J. Schütte ^{aq},
 J. Schwenke ^s, G. Schwering ^s, C. Sciacca ^f, I. Scott ^{aq}, R. Sehgal ⁱ, P.G. Seiler ^{al}, J.C. Sens ^z,
 L. Servoli ^h, I. Sheer ^{aa}, D.Z. Shen ^{am}, S. Shevchenko ^{ap}, X.R. Shi ^{ap}, E. Shumilov ^p,
 V. Shoutko ^p, E. Soderstrom ^u, A. Sopczak ^{aa}, C. Spartiotis ^c, T. Spickermann ^s, P. Spillantini ^b,
 R. Starosta ^s, M. Steuer ^{o,k}, D.P. Stickland ^u, F. Sticozzi ^k, H. Stone ^w, K. Strauch ^{aq},
 B.C. Stringfellow ^{ae}, K. Sudhakar ^{r,s}, G. Sultanov ^l, R.L. Sumner ^u, L.Z. Sun ^{ai,i}, H. Suter ^j,
 R.B. Sutton ^{ab}, J.D. Swain ^l, A.A. Syed ^l, X.W. Tang ^{ah}, L. Taylor ^g, C. Timmermans ^{ak},
 Samuel C.C. Ting ^k, S.M. Ting ^k, M. Tonutti ^s, S.C. Tonwar ^r, J. Tóth ^{y,a}, A. Tsaregorodtsev ^m,
 G. Tsipolitis ^{ab}, C. Tully ^{ap}, K.L. Tung ^{ah}, J. Ulbricht ^j, L. Urbán ^s, U. Uwer ^s, E. Valente ^l,
 R.T. Van de Walle ^{ak}, I. Vetlitsky ^p, G. Viertel ^j, P. Vikas ⁱ, U. Vikas ^l, M. Vivargent ^x,
 H. Vogel ^{ab}, H. Vogt ^{an}, G. Von Dardel ^a, I. Vorobiev ^p, A.A. Vorobyov ^m, L. Vuilleumier ^{ao},
 M. Wadhwa ⁱ, W. Wallraff ^s, C.R. Wang ^{ai}, G.H. Wang ^{ab}, J.H. Wang ^{ah}, Q.F. Wang ^{aq},
 X.L. Wang ^{ai}, Y.F. Wang ^b, Z.M. Wang ^{ia,i}, A. Weber ^s, J. Weber ^j, R. Weill ^{ao}, T.J. Wenaus ^{af},
 J. Wenninger ^w, M. White ^k, C. Willmott ^c, F. Wittgenstein ^a, D. Wright ^u, R.J. Wu ^{ah}, S.X. Wu ⁱ,
 Y.G. Wu ^{ah}, B. Wyslouch ^k, Y.Y. Xie ^{am}, Y.D. Xu ^{ah}, Z.Z. Xu ^{ai}, Z.L. Xue ^{am}, D.S. Yan ^{am},
 X.J. Yan ^k, B.Z. Yang ^{ai}, C.G. Yang ^{ah}, G. Yang ^l, K.S. Yang ^{ah}, Q.Y. Yang ^{ah}, Z.Q. Yang ^{am},
 C.H. Ye ⁱ, J.B. Ye ^{ai}, Q. Ye ⁱ, S.C. Yeh ^{ag}, Z.W. Yin ^{am}, J.M. You ^l, N. Yunus ⁱ, M. Yzerman ^z,
 C. Zaccardelli ^{ap}, P. Zemp ^j, M. Zeng ^l, Y. Zeng ^s, D.H. Zhang ^z, Z.P. Zhang ^{ai,i}, B. Zhou ^d,
 J.F. Zhou ^s, R.Y. Zhu ^{ap}, H.L. Zhuang ^{ah} and A. Zichichi ^{o,a,i}

^a European Laboratory for Particle Physics, CERN, CH-1211 Geneva 23, Switzerland

^b INFN Sezione di Firenze and University of Florence, I-50125 Florence, Italy

^c Centro de Investigaciones Energeticas, Medioambientales y Tecnológicas, CIEMAT, E-28040 Madrid, Spain

^d Boston University, Boston, MA 02215, USA

^e Johns Hopkins University, Baltimore, MD 21218, USA

^f INFN - Sezione di Napoli and University of Naples, I-80125 Naples, Italy

^g Northeastern University, Boston, MA 02115, USA

^h INFN-Sezione di Perugia and Università Degli Studi di Perugia, I-06100 Perugia, Italy

ⁱ World Laboratory, FBLJA Project, CH-1211 Geneva 23, Switzerland

^j Eidgenössische Technische Hochschule, ETH Zürich, CH-8093 Zürich, Switzerland

^k Massachusetts Institute of Technology, Cambridge, MA 02139, USA

^l Iowa State University, Ames, IA 50011, USA

^m Nuclear Physics Institute, St. Petersburg, Russia

ⁿ Bulgarian Academy of Sciences, Institute of Mechatronics, BU-1113 Sofia, Bulgaria

- ^o INFN-Sezione di Bologna, I-40126 Bologna, Italy
- ^p Institute of Theoretical and Experimental Physics, ITEP, SU-117259 Moscow, Russia
- ^q University of Michigan, Ann Arbor, MI 48109, USA
- ^r Tata Institute of Fundamental Research, Bombay 400005, India
- ^s I. Physikalisches Institut, RWTH, W-5100 Aachen, FRG ²
- III. Physikalisches Institut, RWTH, W-5100 Aachen, FRG ²
- ^t INFN-Sezione di Roma and University of Roma, "La Sapienza", I-00185, Rome, Italy
- ^u Princeton University, Princeton, NJ 08544, USA
- ^v University of Alabama, Tuscaloosa, AL 35486, USA
- ^w University of Geneva, CH-1211 Geneva 4, Switzerland
- ^x Laboratoire de Physique des Particules, LAPP, F-74519 Annecy le Vieux, France
- ^y Central Research Institute for Physics of the Hungarian Academy of Sciences, H-1525 Budapest 114, Hungary
- ^z National Institute for High Energy Physics, NIKHEF, NL-1009 DB Amsterdam, The Netherlands
- ^{aa} University of California, San Diego, CA 92182, USA
- ^{ab} Carnegie Mellon University, Pittsburgh, PA 15213, USA
- ^{ac} Los Alamos National Laboratory, Los Alamos, NM 87544, USA
- ^{ad} Institut de Physique Nucléaire de Lyon, IN2P3-CNRS/Université Claude Bernard, F-69622 Villeurbanne Cedex, France
- ^{ae} Purdue University, West Lafayette, IN 47907, USA
- ^{af} Lawrence Livermore National Laboratory, Livermore, CA 94550, USA
- ^{ag} High Energy Physics Group, Taiwan, ROC
- ^{ah} Institute of High Energy Physics, IHEP, Beijing, PR China
- ^{ai} Chinese University of Science and Technology, USTC, Hefei, Anhui 230029, PR China
- ^{aj} Oak Ridge National Laboratory, Oak Ridge, TN 37831, USA
- ^{ak} University of Nymegen and NIKHEF, NL-6525 ED Nymegen, The Netherlands
- ^{al} Paul Scherrer Institut, PSI, CH-5232 Villigen, Switzerland
- ^{am} Shanghai Institute of Ceramics, SIC, Shanghai, PR China
- ^{an} Institut für Hochenergiephysik, O-1615 Zeuthen, FRG ²
- ^{ao} University of Lausanne, CH-1015 Lausanne, Switzerland
- ^{ap} California Institute of Technology, Pasadena, CA 91125, USA
- ^{aq} Harvard University, Cambridge, MA 02139, USA
- ^{ar} Department of Natural Sciences, University of Cyprus, Nicosia, Cyprus
- ^{as} University of Hamburg, W-2000 Hamburg, FRG

Received 18 March 1992

Dedicated to the memory of Professor Prince K. Malhotra

A search for the standard model neutral Higgs boson is described. Data collected during 1990 and 1991, corresponding to 408 000 hadronic decays of the Z^0 , were used. At the 95% confidence level we exclude the existence of the minimal standard model Higgs boson in the mass range $0 \leq M_{H^0} < 52$ GeV.

1. Introduction

In the minimal standard model, the Higgs mechanism is responsible for the mass generation of the W^\pm and Z^0 vector bosons [1,2] and the existence of a neutral spinless Higgs particle H^0 is predicted. In this model the couplings of the H^0 boson to the fermions

and the vector bosons are known but its mass is not specified.

At centre of mass energies near the Z^0 peak the main Higgs boson production mode is predicted to be through the Z^0 boson decay into a H^0 and a virtual Z^{0*} [3]:

$$e^+e^- \rightarrow Z^0 \rightarrow H^0 + Z^{0*} \rightarrow H^0 + f\bar{f}.$$

We have previously reported on searches for the standard model Higgs boson using the 1990 data sample, corresponding to 5.3 pb^{-1} integrated lumi-

¹ Supported by the German Bundesministerium für Forschung und Technologie.

² Deceased.

nosity around the Z^0 pole [4,5]. These searches allowed us to exclude the presence of the Higgs boson in the mass range $0 \leq M_{H^0} < 41.8$ GeV at the 95% confidence level. Searches have also been performed by the other LEP experiments [6–8].

We have expanded the search for the H^0 by including our 1991 data sample, corresponding to 292 000 Z^0 hadronic decays. Combined with the 1990 data this totals 408 000 Z^0 hadronic decays and 17.5 pb^{-1} integrated luminosity at centre of mass energies between 88.2 and 94.3 GeV.

Here we report on our search for the Higgs boson in the mass range from 30 to 60 GeV. We have searched in the channels: $H^0 \nu \bar{\nu}$, $H^0 e^+ e^-$, $H^0 \mu^+ \mu^-$, $(H^0 \rightarrow \tau^+ \tau^-)(Z^{0*} \rightarrow q \bar{q})$ and $(H^0 \rightarrow q \bar{q})(Z^{0*} \rightarrow \tau^+ \tau^-)$.

2. The L3 detector

The L3 detector consists of a central tracking chamber, a high resolution electromagnetic calorimeter composed of BGO crystals, a ring of scintillation counters, a uranium and brass hadron calorimeter with proportional wire chamber readout, and an accurate muon chamber system. These detectors are installed in a 12 m diameter magnet which provides a uniform field of 0.5 T along the beam direction. For hadronic jets the fiducial coverage is 99% of 4π .

The central tracking chamber (TEC) is a time expansion chamber which consists of two cylindrical layers of 12 (inner) and 24 (outer) sectors, with 62 wires measuring the R - ϕ coordinate. The single wire resolution is $58 \mu\text{m}$ averaged over the entire cell. The double-track resolution is $640 \mu\text{m}$. The BGO electromagnetic calorimeter, which now includes endcaps installed in 1991, covers 85% of the solid angle. The fine segmentation of the BGO detector and hadron calorimeter allows us to measure the direction of jets with an angular resolution of 2.1° , and to measure the total energy of hadronic events from Z^0 decay with a resolution of 10.2%. The muon detector consists of three layers of precise drift chambers, which measure 56 points on the muon trajectory in the bending plane, and 8 points in the non-bending direction.

We have previously described the detector and its performance in detail [9,10].

3. Simulation and data analysis

In order to establish the selection criteria and to evaluate the selection efficiency a Monte Carlo simulation of different processes has been carried out.

Hadronization and decays were simulated using the program JETSET 7.3 [11] with parton shower fragmentation. The response of the detector was simulated using the L3 detector simulation program ^{#1} which takes into account the effects of energy loss, multiple scattering, interactions and decays and includes the detector efficiency and resolution.

Higgs events were generated in the $H^0 \nu \bar{\nu}$, $H^0 e^+ e^-$, $H^0 \mu^+ \mu^-$ and both $\tau^+ \tau^- q \bar{q}$ channels in the H^0 mass range from 30 to 60 GeV. The event generator program includes initial state photon radiation and final state radiation of photons from leptons and gluons from quarks. In this mass range the Higgs boson predominantly decays into a $b \bar{b}$ pair. The branching ratios into $c \bar{c}$ and $\tau^+ \tau^-$ are not negligible [14] and were included. With QCD corrections [15] the branching ratio into $\tau^+ \tau^-$ for a 50 GeV Higgs boson is approximately 5.5%.

The samples of Monte Carlo events used in the present analysis are: 647 000 Z^0 hadronic decays including 165 000 for the 1990 setup, 85 000 $\tau^+ \tau^-$ events, 1000 H^0 events at different masses for each decay channel and 500 four fermion events [16] of the types $q \bar{q} \ell^+ \ell^-$ for each combination of the different quarks and leptons.

As the selections described below extensively use the information coming from the calorimetric part of the detector, we briefly describe the related reconstruction algorithm. Jets are reconstructed using a two step procedure [10]: firstly neighbouring calorimetric hits are combined into clusters, then jets are formed merging neighbouring clusters and muon tracks. Each charged track measured in the tracking chamber is assigned to the nearest jet. The algorithm normally reconstructs one such "jet" for a single isolated electron, photon, muon, high energy τ or a hadronic jet. Unless otherwise stated in the following jets are defined by this algorithm.

The trigger efficiency for the studied signal is in ex-

^{#1} The L3 detector simulation is based on GEANT Version 3.14, see ref. [12]. The GHEISHA program is used to simulate hadronic interactions, see ref. [13].

cess of 99.9% for all the channels in the Higgs boson mass range under study.

4. $H^0\nu\bar{\nu}$ event selection

$H^0\nu\bar{\nu}$ events are characterized by large missing energy and momentum imbalance due to the undetected neutrinos from the Z^{0*} decay. The heavy quarks from the Higgs decay receive a Lorentz boost leading to two acoplanar jets which mainly populate one hemisphere with a rather low energy deposit in the other. The direction of the missing energy, being mainly that of the Z^{0*} , is far from the quark jets. In contrast, in the $e^+e^- \rightarrow q\bar{q}$ events (the main source of background in this mass range), the two jets from the $q\bar{q}$ system are typically coplanar with the beam axis, seldom leading to low energy deposits in any one hemisphere. The relatively small missing energy is mostly due to the undetected neutrinos within the jets or to the jet energy resolution, as a consequence the missing energy direction is close to one of the jet axes.

The search for Higgs candidates is carried out taking advantage of the above signatures.

In the preselection a set of cuts is applied to eliminate a large fraction of the background due to the $q\bar{q}$, $\tau^+\tau^-$, two photon processes, cosmic rays and beam gas interactions. We require the following:

- The invariant mass of all the calorimetric clusters (assumed to be massless), M_{vis} , is within the range 25–65 GeV.
- The energy imbalance transverse to the beam axis is larger than 15% and that parallel to the beam axis is less than 45% of the visible energy. The direction of the energy imbalance is more than 0.4 rad away from the beam axis.
- There are more than four charged tracks with transverse momenta larger than 0.3 GeV and with distances of closest approach to the beam axis less than 5 mm. There are more than 12 calorimetric clusters.

The acceptance of the above cuts for $H^0\nu\bar{\nu}$ events with M_{H^0} of 50 GeV is 79% and we are left with 0.85% of the Z^0 hadronic decays, the background from all other sources being negligible. The visible mass distribution for the remaining events is shown in fig. 1.

For the final selection we use a set of cuts which are designed to reject all events from the background channels in the existing Monte Carlo samples while

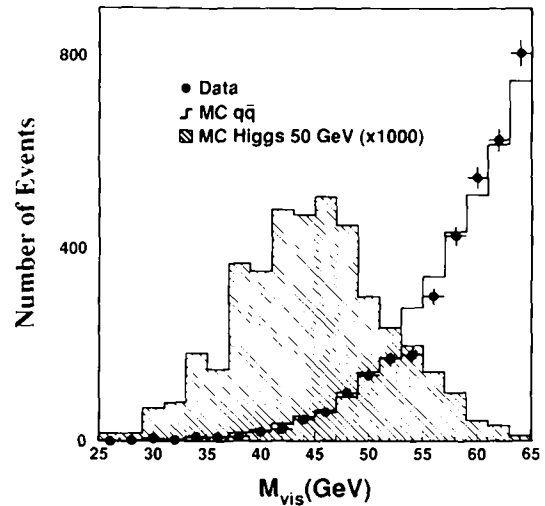


Fig. 1. Visible mass distribution for the data, simulated $q\bar{q}$ background and Higgs signal ($M_{H^0} = 50$ GeV) which pass the preselection for the $H^0\nu\bar{\nu}$ search. Background Monte Carlo events are normalized to the total integrated luminosity. The signal has been multiplied by 1000 for visibility.

maintaining a high detection efficiency for the Higgs boson. All these cuts are based on topological variables which are mostly related to the jet axis measurement. The jet directions are usually well defined even for events with large missing energy. The jet reconstruction starts by identifying the two calorimetric clusters that have the largest invariant mass. The plane perpendicular to that containing the direction vectors of the two clusters and bisecting the angle defined by them divides the event into two hemispheres. All the clusters in each hemisphere are combined to form a jet whose direction is determined by adding the momentum vectors of the clusters. Hence we obtain exactly two jets for each event, corresponding to the primary $q\bar{q}$ pair. Finally we define a unit vector \hat{h} which is opposite to the sum of the unit vectors along the two jet directions.

An event is accepted if it satisfies the following criteria:

- (1) $E_{90} < 10$ GeV and $E_{60} < 3$ GeV, where E_{90} and E_{60} are the energies deposited in the cones with half opening angles of 90° and 60° respectively around \hat{h}
- (2) The largest angular region in the $R-\phi$ plane where no tracks are present must be greater than 1.1 rad.
- (3) $E_1 < 1$ GeV, where E_1 is the energy deposited in

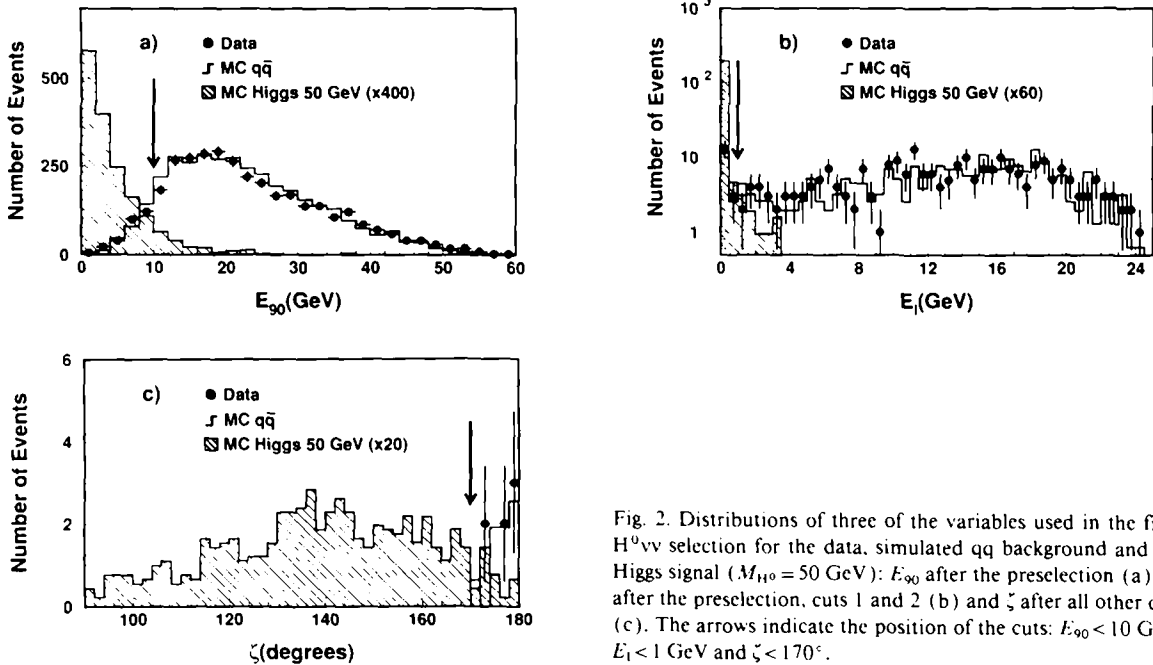


Fig. 2. Distributions of three of the variables used in the final $H^0\nu\nu$ selection for the data, simulated $q\bar{q}$ background and the Higgs signal ($M_{H^0} = 50$ GeV): E_{90} after the preselection (a), E_1 after the preselection, cuts 1 and 2 (b) and ζ after all other cuts (c). The arrows indicate the position of the cuts: $E_{90} < 10$ GeV, $E_1 < 1$ GeV and $\zeta < 170^\circ$.

a cone of 20° half opening angle around the missing energy direction.

(4) $\xi < 160^\circ$ and $\zeta < 170^\circ$, where ξ and ζ are the angles between the two jets in space and in the $R-\phi$ plane respectively.

Figs. 2a-2c show the distributions of E_{90} , E_1 and ζ respectively, for the 50 GeV Higgs Monte Carlo events, $q\bar{q}$ Monte Carlo and the data before the cut in that variable is applied.

The detection efficiency for the Higgs signal as a function of the H^0 mass is shown in table 1.

The uncertainty in the selection efficiency has been studied by changing the detector calibration constants within their errors and by using two different hadronization models in the Monte Carlo. The effect of the changes in the calibration were found to be less than 1.5% of the detection efficiency for a 50 GeV Higgs mass. The selection efficiencies for the same

Table 1

Selection efficiencies (in %) for Higgs events in the different channels. The efficiencies for the $H^0\nu\nu$ and $H^0\mu^+\mu^-$ channels are the same for 1990 and 1991 data.

	Higgs mass (GeV)				
	30	40	50	55	60
$H^0\nu\nu$ channel	36.4	60.6	59.0	50.3	37.4
$H^0e^+e^-$ channel (1991)	58.2	55.2	52.2	50.5	49.4
$H^0e^+e^-$ channel (1990)	45.5	38.0	35.0	32.0	29.0
$H^0\mu^+\mu^-$ channel	62.6	61.2	61.6	60.6	55.4
$(H^0 \rightarrow \tau^+\tau^-)(Z^0 \rightarrow q\bar{q})$ (1991)	3.8	10.2	15.8	17.6	15.0
$(H^0 \rightarrow q\bar{q})(Z^0 \rightarrow \tau^+\tau^-)$ (1991)	14.6	8.6	4.0	2.2	1.4
$(H^0 \rightarrow \tau^+\tau^-)(Z^0 \rightarrow q\bar{q})$ (1990)	2.4	5.4	9.4	12.4	8.8
$(H^0 \rightarrow q\bar{q})(Z^0 \rightarrow \tau^+\tau^-)$ (1990)	8.0	4.2	2.2	1.4	1.2

mass using JETSET 7.3 and HERWIG 5.3 [17] agree well within the statistical errors. We also repeated the study of $q\bar{q}\gamma$ events which have a similar topology to the $H^0\nu\bar{\nu}$ signal after eliminating the γ from the reconstruction [5]. For these event we compared all the variables used in the analysis and found good agreement between data and Monte Carlo. From these studies we conclude that our efficiencies are affected by a relative uncertainty of less than 1.5%.

No events pass our selection cuts.

Using the 1991 data sample we also repeated the $H^0\nu\bar{\nu}$ analysis that had been performed for the 1990 data [5]; the analysis was slightly modified [18] in order to increase the efficiency for higher Higgs boson masses. This analysis also found no candidates in the mass range from 30 to 60 GeV with an efficiency for the signal of 54% at 50 GeV.

5. $H^0e^+e^-$ event selection

The distinctive signature of this process is the presence of two energetic and well separated electrons coming from the virtual Z^0 isolated from the H^0 decay products. The main sources of background are the four fermion process $e^+e^- \rightarrow e^+e^- q\bar{q}$ and the double semileptonic decay $Z^0 \rightarrow b\bar{b} \rightarrow e^+e^- X$.

In our selection low multiplicity events, such as e^+e^- and $\tau^+\tau^-$ final states, are removed by requiring at least 15 clusters in the electromagnetic calorimeter.

To reduce the hadronic background in our sample we require that the two most energetic clusters have energies greater than 3 GeV and that the sum of their energies exceeds 15 GeV; in addition the opening angle between these two clusters must be larger than 40° .

The identification of electromagnetic particles is mainly based on the energy deposition pattern in the electromagnetic calorimeter. We consider the ratio of the energy deposited in a 3×3 crystal array and the energy deposited in a 5×5 array both centered on the most energetic crystal in the cluster. After applying a position-dependent leakage correction to both measurements the distribution of this ratio is approximately gaussian, centered at 1.0 with a width of 1%. Electromagnetic candidates are identified by requiring that this ratio is less than 3σ away from the above mean value.

The isolation of the electron candidates is further

ensured by imposing the following conditions:

- The additional energy deposited in the electromagnetic calorimeter in a cone of 15° opening angle around the direction of the highest energy cluster must not exceed 5% of the cluster energy and the energy measured in the hadron calorimeter in the same cone must be less than 3 GeV.
- The additional energy deposited in the electromagnetic calorimeter in a cone of 15° opening angle around the second most energetic cluster must not exceed 7% of its energy.

To complete the identification of the electrons we require the most energetic cluster to match in azimuthal angle with exactly one track and the second most energetic cluster with at least one track. For both clusters the matching has to be within a 4σ cut where σ depends on the energies and on the polar angles of the clusters.

To identify the Higgs boson decay products we examine the non-electron jets in the event. Indicating with P_\perp the transverse momentum of each electron with respect to the nearest jet, we require the sum of the two P_\perp 's to be larger than 10 GeV. If only one jet

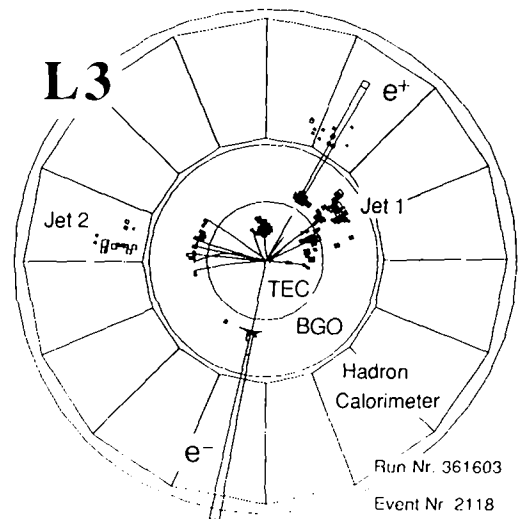


Fig. 3. The 31.4 GeV mass candidate found in the $H^0e^+e^-$ channel shown in the plane perpendicular to the beam line. The lines in the TEC represent the reconstructed charged tracks. The size of the symbols indicating individual calorimetric hits (towers in the BGO electromagnetic calorimeter and boxes in the hadron calorimeter) corresponds to the energy deposition in that hit. The towers which appear in the TEC region in this projection belong to the BGO endcaps.

Table 2

The energies (E), the polar angles with respect to the beam line (θ) and the azimuthal angles (ϕ) of the main constituents of the $H^0 e^+ e^-$ candidate are indicated. The main parameters of the event are: $\sqrt{s} = 88.4$ GeV, missing mass recoiling against the final state $e^+ e^- = 31.4 \pm 1.5$ GeV, mass ($e^+ e^-$) $= 46.8 \pm 1.9$ GeV, measured mass of the hadronic system $= 23$ GeV; this last value is consistent with the Monte Carlo expectation of 28.7 ± 4.3 GeV for a Higgs boson with mass 31.4 GeV.

	E (GeV)	θ (deg.)	ϕ (deg.)
jet ₁	23.8	152.8	47.5
jet ₂	9.4	101.4	173.4
e^+	25.95 ± 1.0	35.8	59.9
e^-	25.13 ± 0.35	99.6	258.5

is present we require the sum of the two P_{\perp} 's to be larger than 30 GeV.

The selection efficiencies for the signal are shown in table 1 for the 1990 and 1991 setup. The efficiency for the 1990 data is lower due to the lower geometrical acceptance of the BGO calorimeter which did not include the endcaps.

One event passed the above selection criteria: the missing mass recoiling against the electron pair is 31.4 ± 1.5 GeV. The event is shown in fig. 3 and its main parameters are given in table 2. This event is consistent with the four fermion background from which we expect 1.6 ± 0.3 events.

No events pass our selection in samples of 340 000 $q\bar{q}$ and 70 000 $\tau^+ \tau^-$ Monte Carlo events. We have also simulated $Z^0 \rightarrow b\bar{b} \rightarrow e^- e^- X$ events corresponding to $1.6 \times 10^6 e^+ e^- \rightarrow$ hadrons and no events passed our selection.

6. $H^0 \mu^+ \mu^-$ event selection

This analysis is based on the selection of events with well isolated muons together with other charged particles present in the fragmentation of the heavy quark pair from the Higgs decay.

The selection is based on tracks in the muon spectrometer that when extrapolated back towards the beam line pass within 3.5σ from the interaction point, both in the R - ϕ and z directions; in the following we refer to these muon tracks simply as muons.

We require the presence of at least one muon satisfying these criteria. Furthermore, we require at least five tracks to be reconstructed in the TEC in order to remove cosmic ray, $\mu^+ \mu^-$, $\tau^+ \tau^-$, $e^+ e^- \mu^+ \mu^-$ and $\pi^+ \pi^- \mu^+ \mu^-$ events. In order to reduce the background from $Z^0 \rightarrow q\bar{q}$ events, we require the event thrust to be less than 0.92.

Two sets of cuts are applied: set (i) to recognize a single well isolated muon and set (ii) to select the muon pair from the Z^{0*} decay. An event passes the selection if it has at least one muon surviving the first set of cuts (i) or at least one muon pair surviving the second set of cuts (ii). This allows us to recover the events in which one of the two muons coming from the decay of the virtual Z^0 is not detected in the muon spectrometer.

To measure the isolation of a muon we define the quantity \mathcal{I} :

$$\mathcal{I}_i = \frac{E_{\text{jet}_i} - p_{\mu_i}}{p_{\mu_i}},$$

where E_{jet_i} is the energy of the jet which includes the i th muon and p_{μ_i} is the value of the muon momentum.

The two sets of cuts are the following:

Set (i). In order to reduce the large background due to the semileptonic decays of hadrons into low momentum muons, the muon must have a momentum larger than 10 GeV. To ensure the isolation, we require less than six calorimetric clusters and at most one additional charged track in the jet which includes the muon. The isolation parameter \mathcal{I} must have a value of less than 0.3.

Set (ii). To identify a muon pair from the decay of the Z^{0*} the following isolation cuts are applied:

- There should be at least one muon with less than six calorimetric clusters in the associated jet.
- There should be at least one muon with less than five charged tracks in the associated jet.
- There should be at least one muon separated by more than 0.4 rad from the axis of the nearest jet which does not include any of the muons.
- $\mathcal{I}_1 \cdot \mathcal{I}_2 < 1.5$.

To reduce the background from the semileptonic decays of hadrons the following cuts are used;

- $\min(p_{\mu_1}, p_{\mu_2}) > 3.4$ GeV and $p_{\mu_1} + p_{\mu_2} > 12$ GeV.
- The invariant mass of the muon pair must be larger than 1 GeV.

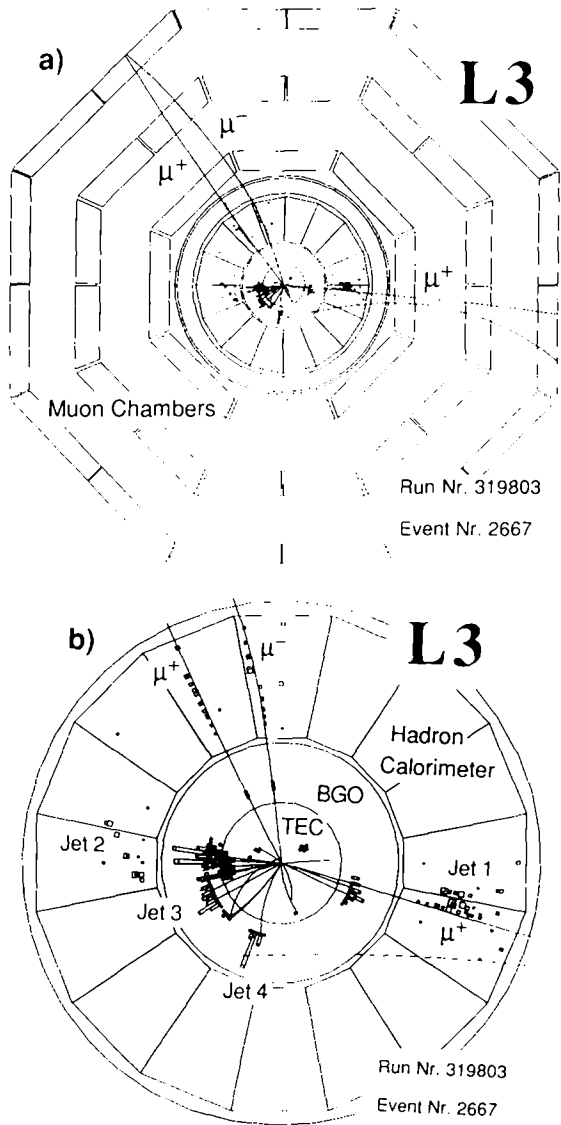


Fig. 4. The 70.4 GeV mass candidate found in the $H^0\mu^+\mu^-$ channel shown in the plane perpendicular to the beam line. (a) shows the whole detector, including the muon chambers. (b) shows the central region. The lines in the TEC represent the reconstructed charged tracks. The size of the symbols indicating individual calorimetric hits (towers in the BGO electromagnetic calorimeter and boxes in the hadron calorimeter) corresponds to the energy deposition in that hit. The towers which appear in the TEC region in this projection belong to the BGO endcaps. In (a) the muon tracks can be seen as reconstructed in the three layers of chambers. The track in the muon chambers which, when extrapolated back (dashed line), passes far away from the interaction point is most likely due to a "punch through" particle.

Table 3

The energies (E), the polar angles with respect to the beam line (θ) and the azimuthal angles (ϕ) of the main constituents of the $H^0\mu^+\mu^-$ candidate are indicated. The main parameters of the event are: $\sqrt{s}=91.3$ GeV, missing mass recoiling against $\mu^+\mu^- = 70.4 \pm 0.7$ GeV, mass ($\mu^+\mu^-$) = 6.5 ± 0.2 GeV, measured mass of the hadronic system = 61.6 GeV; this last value is consistent with the Monte Carlo expectation of 65.7 ± 6.2 GeV for a Higgs boson with mass 70.4 GeV.

	E (GeV)	θ (deg.)	ϕ (deg.)
jet ₁	25.7	128.8	354.6
jet ₂	23.6	34.9	189.3
jet ₃	8.6	84.5	212.8
jet ₄	4.9	127.9	261.8
μ^-	14.9 ± 0.55	50.5	128.7
μ^+	3.80 ± 0.15	98.0	107.6
μ^+ in jet ₁	14.6 ± 0.59	126.7	355.4

The selection efficiencies for the Higgs signal are shown in table 1.

One event passed the above selection criteria: the missing mass recoiling against the two well isolated muons is 70.4 ± 0.7 GeV. The event is shown in fig. 4 and its main parameters are given in table 3. This event is consistent with the four fermion background from which we expect 1.7 ± 0.2 events.

No events pass our selection in samples of 340 000 $q\bar{q}$ and 70 000 $\tau^+\tau^-$ Monte Carlo events.

7. $\tau^+\tau^- q\bar{q}$ event selection

The search for the Higgs signal with τ leptons in the final state was performed using the two channels: $(H^0 \rightarrow \tau^+\tau^-)(Z^{0*} \rightarrow q\bar{q})$ and $(H^0 \rightarrow q\bar{q})(Z^{0*} \rightarrow \tau^+\tau^-)$. The selection was optimized for a 55 GeV Higgs boson in the configuration $(H^0 \rightarrow \tau^+\tau^-)(Z^{0*} \rightarrow q\bar{q})$, which is predicted to have the highest cross section among all the possible Higgs channels with τ leptons.

As the $\tau^+\tau^- q\bar{q}$ final state produces mostly four jets we require the presence of at least three and at most five jets.

In order to remove most $q\bar{q}, \tau^+\tau^-$ events, two photon processes and beam gas interactions, we require the following:

- The visible energy is between 30 and 65 GeV and the most energetic jet has an energy less than 35 GeV.

- The energy imbalance transverse to the beam axis is larger than 5% and that parallel to the beam axis is less than 30% of the visible energy.
- The major is greater than 0.3, where the major is defined as the maximum value of the quantity $(\sum_i \mathbf{E}_i \cdot \hat{p}) / (\sum_i |\mathbf{E}_i|)$ when the vector \hat{p} is contained in the plane perpendicular to the thrust axis. \mathbf{E}_i indicates the energy and the direction of each calorimetric cluster and the index i runs over all the clusters in the event.
- There are at least 14 calorimetric clusters and at most 21 tracks.

In order to identify the τ decay products we require the following:

- At least two "tau" jets, defined as narrow jets (jet thrust greater than 0.99) which form an angle of at least 10° with the beam direction and contain less than six tracks and less than ten calorimetric clusters each. For 1990 data, due to the lower acceptance of the BGO calorimeter, we require the "tau" jet directions to be at least 45° away from the beam direction.
- At least one isolated track, defined as a track with a momentum greater than 3 GeV, matched with a calorimetric cluster of energy larger than 1 GeV within a 6° half opening angle cone around the track direction and with no other tracks in a 15° half opening angle cone. The isolated track can be one of the above required "tau" jets.

Finally we require that the energy outside the two most energetic "tau" jets is less than 40 GeV.

No events survive this selection both in the data and in samples of 340 000 $q\bar{q}$ and 40 000 $\tau^+\tau^-$ Monte Carlo events. Less than 0.1 events are expected from $e^+e^- \rightarrow \tau^+\tau^- q\bar{q}$ processes.

The detection efficiencies corresponding to the 1990 and 1991 data for different Higgs masses are shown in table 1.

8. Systematic uncertainties

The sources of systematic errors on the number of expected Higgs events are the following

- Theoretical uncertainty of less than 1% on the ratio between the Higgs boson production cross section and the $e^+e^- \rightarrow q\bar{q}$ cross section [19].
- Experimental uncertainty of 0.5% on the corrected number of Z^0 hadronic decays used for the normalization [20].

- Theoretical uncertainty on the Higgs decay branching ratios which contributes an error of 1% to the detection efficiency.

- Error on the Higgs detection efficiency of 1.5% due to the uncertainties in the Monte Carlo fragmentation parameters, estimated by changing the fragmentation model and varying the detector calibration constants.

- Error on the Higgs detection efficiency of 1.5% due to Monte Carlo statistics.

Combining all these errors in quadrature we obtain an overall systematic uncertainty of 2.6%.

9. Mass limit

From a total of 408 000 hadronic events, we have observed one e^+e^- hadrons and one $\mu^+\mu^-$ hadrons event that pass our selection criteria. From Monte Carlo studies, we expect the background in the Higgs search from four fermion processes to be 1.6 ± 0.3 $e^+e^- q\bar{q}$ events for the $H^0 e^+e^-$ channel and 1.7 ± 0.2 $\mu^+\mu^- q\bar{q}$ events for the $H^0 \mu^+\mu^-$ channel. Neither event is consistent with a Higgs boson mass in the vicinity of 50 GeV. Therefore we take the 95% confidence level limit on the Higgs boson mass corresponding to three events. Taking into account the

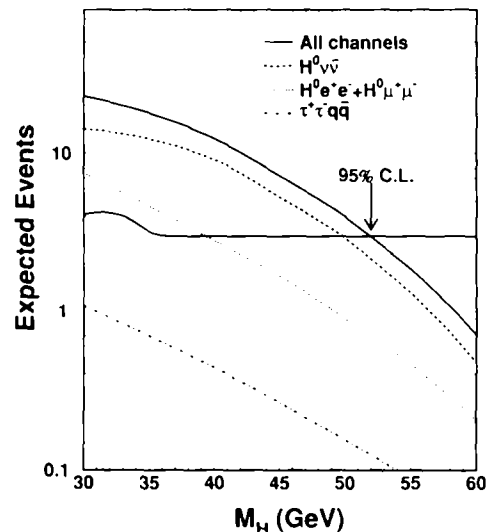


Fig. 5. Number of events expected in the different channels. The 95% confidence level line is shown and the Higgs mass limit at the 95% CL is indicated.

2.6% systematic error on the number of expected events we obtain a 95% CL lower limit on the mass of the Higgs boson of 52 GeV.

Fig. 5 shows the number of expected events in the mass range from 30 to 60 GeV. The 95% CL line, also shown in the figure, was obtained with the likelihood function of the two candidates, taking into account the number of expected events from the background and from the signal and the experimental mass measurement errors.

Acknowledgement

We wish to express our gratitude to the CERN accelerator divisions for the excellent performance of the LEP machine. We acknowledge the efforts of all engineers and technicians who have participated in the construction and maintenance of this experiment.

References

- [1] S.L. Glashow, Nucl. Phys. 22 (1961) 579;
S. Weinberg, Phys. Rev. Lett. 19 (1967) 1264;
A. Salam, Elementary particle theory, ed. N. Svartholm (Almqvist and Wiksell, Stockholm, 1968) p. 367.
- [2] P.W. Higgs, Phys. Lett. 12 (1964) 132; Phys. Rev. Lett. 13 (1964) 508; Phys. Rev. 145 (1966) 1156;
F. Englert and R. Brout, Phys. Rev. Lett. 13 (1964) 321.
- [3] B.L. Ioffe and V.A. Khoze. What can be expected from experiments on colliding e^+e^- beams with ≈ 100 GeV?. LINP preprint (Leningrad, November 1976);
J.D. Bjorken, Proc. 1976 SLAC Summer Institute on Particle physics (Stanford), ed. M. C. Zipf (Stanford Linear Accelerator Center, Stanford, CA, 1977) p. 1;
J. Finjord, Phys. Scr. 21 (1980) 143.
- [4] L3 Collab., B. Adeva et al., Phys. Lett. B 248 (1990) 203; B 252 (1990) 518.
- [5] L3 Collab., B. Adeva et al., Phys. Lett. B 257 (1991) 450.
- [6] ALEPH Collab., D. Decamp et al., Phys. Lett. B 236 (1990) 233; B 241 (1990) 141; B 245 (1990) 289; B 246 (1990) 306; preprint CERN-PPE/91-149 (1991), Phys. Rep., to be published.
- [7] DELPHI Collab., P. Abreu et al., Nucl. Phys. B 342 (1990) 1; B 373 (1992) 3; Z. Phys. C 51 (1991) 25; preprint CERN-PPE/91-132 (1991).
- [8] OPAL Collab., M.Z. Akrawy et al., Phys. Lett. B 236 (1990) 224; B 251 (1990) 211; B 253 (1991) 511; Z. Phys. C 49 (1990) 1;
OPAL Collab., P.D. Acton et al., Phys. Lett. B 268 (1991) 122.
- [9] L3 Collab., B. Adeva et al., Nucl. Instrum. Methods A 289 (1990) 35.
- [10] O. Adriani et al., Nucl. Instrum. Methods A 302 (1991) 53.
- [11] T. Sjöstrand and M. Bengtsson, Comput. Phys. Commun. 43 (1987) 367;
T. Sjöstrand, in: Z Physics at LEP1, CERN report CERN-89-08, Vol. 3, p. 143.
- [12] R. Brun et al., GEANT 3, CERN DD/EE/84-1 (revised) (September 1987).
- [13] H. Fesefeldt, RWTH Aachen preprint PITHA 85/02 (1985).
- [14] P.J. Franzini et al., in: Z Physics at LEP1, CERN report CERN-89-08, eds. G. Altarelli, R. Kleiss and C. Verzegnassi (CERN, Geneva, 1989) Vol. 2, p. 59 and references therein.
- [15] E. Braaten and J.P. Leveille, Phys. Rev. D 22 (1980) 715.
- [16] E.W.N. Glover, R. Kleiss and J.J. van der Bij, Z. Phys. C 47 (1990) 435.
- [17] G. Marchesini and B. Webber, Nucl. Phys. B 310 (1988) 461;
I.G. Knowles, Nucl. Phys. B 310 (1988) 571.
- [18] H. Akbari et al., A search for the neutral Higgs boson in $H^0\nu\nu$ channel, L3 internal note 1117 (1992).
- [19] M. Consoli and W. Hollik, in: Z Physics at LEP1, CERN report CERN-89-08, eds. G. Altarelli, R. Kleiss and C. Verzegnassi (CERN, Geneva, 1989) Vol. 1, p. 39;
B.A. Kniehl, Radiative corrections to Higgs production from Z^0 decay, preprint DESY 92-021 (February 1992);
F.A. Berends, W.L. van Neerven and G.J.H. Burgers, Nucl. Phys. B 297 (1988) 429.
- [20] L3 Collab., B. Adeva et al., Z. Phys. C 51 (1991) 1179.